Binding of Multivalent Ligands to Cells: Effects of Cell and Receptor Density

Condensed title: Binding of Multivalent Ligands

(Keywords: Multivalent Ligands, Crosslinking
Receptor Density, Fc Receptor)

Bernhard Sulzer and Alan. S. Perelson

Theoretical Biology and Biophysics
Los Alamos National Laboratory
Los Alamos, NM 87545, USA

November 23, 1994

Abstract

We study the equilibrium binding properties of multivalent ligands and mixtures of ligands of different valence to cell surface receptors. We examine the effects of changing cell density or number of receptors per cell, i.e., receptor concentration, over a wide but physiologically relevant range. Qualitatively different behaviour arises in the *excess receptor regime*, where the volume concentration of receptors is much greater than the ligand concentration, and the *excess ligand regime*, where the ligand concentration is much greater than the receptor concentration. In the excess receptor regime a ligand binds at as many sites as possible as determined by the crosslinking affinity constant and the valence of the ligand. Thus ligands tend to be bound at many sites. In the excess ligand regime, ligands compete for receptor binding and hence tend to bind at a low number of sites per molecule. However, the total number of ligands bound per cell is higher in the excess ligand regime than at the same total ligand concentration in the excess receptor regime. When cells are exposed to an ensemble of ligand of different valence there is a preference for binding of larger valence ligands both in the excess receptor regime and in the transition range from the excess receptor to the excess ligand regime. Increasing the volume concentration of receptors, say by increasing the cell density, reduces this preference. We apply our theory to the binding of chemically crosslinked oligomers of immunoglobulin to Fc receptors on various cell types. We also examine the binding of haptenated polymers to B cells and reinterpret experiments related to the immunon theory of B cell activation.

1 Introduction

The interaction of multivalent ligand with cell surface receptors underlies many different aspects of cell recognition and response. While both monovalent and multivalent ligands can bind to cell surface receptors, only multivalent ligands have the ability to simultaneously bind multiple receptors, that is to crosslink receptors. The amount of receptor crosslinking as opposed to receptor binding provides signals for many cells of the immune system. On B lymphocytes the crosslinking of bivalent surface immunoglobulin (Ig)-receptors is part of the normal signaling pathway that leads to B cell activation. Crosslinking of the T cell receptor by antibody can trigger T cell activation. Histamine release can be triggered from sensitized basophils and mast cells through the crosslinking of surface IgE, or by the crosslinking of Fc-receptors (FcR) in the membranes of unsensitized cells (Fewtrell and Metzger, 1980). Although not usually thought of as crosslinking, the binding of antigen-antibody complexes to FcR on macrophages is also a crosslinking event that is involved in cell stimulation.

The response of a cell to various crosslinking events may not be the same. The degree of crosslinking and the nature of the cell-bound ligand states may determine the response of the cell. For example, Dintzis et al. (1976) suggests that B cells are only triggered when a critical number of receptors, of the order of 10, are crosslinked. Crosslinking smaller numbers of receptors may lead to tolerance (Dintzis et al., 1983). Antigen-antibody aggregates can interact with B cells in such a way that the antigen binds to Ig receptors and the Fc regions of the antibody in the complex binds to FcR. This has been called co-crosslinking since both Ig and FcR can be simultaneously crosslinked. While crosslinking just the Ig receptor can stimulate cells, co-crosslinking leads to a downregulation of the B cell response (Phillips and Parker, 1983; Phillips and Parker, 1984; Wofsy and Goldstein, 1990).

Here we shall develop and analyze quantitative models of receptor crosslinking. We shall formulate our models in a general way so that they will apply to situations where the crosslinking ligand is a single type of molecule, such as a monoclonal bivalent antibody, or a collection of molecules, such as a set of covalently crosslinked antibody molecules or a set of haptenated polymers in which the degree of haptenization may vary.

In vitro experiments on the binding of ligands to cell receptors and the ensuing signaling events are typically performed with an excess of ligand. The mathematical analyses of those binding processes have thus used what has been called the excess ligand approximation (Perelson and DeLisi, 1980), which greatly simplifies the analysis. Here we shall study binding and crosslinking events that occur for a wide range of concentrations. In some parameter regions the excess ligand approximation will be made. We also introduce a new approximation, the "excess receptor approximation", which plays a role at high cell densities.

The equilibrium binding characteristics of *ensembles* of ligands with different valence but identical affinities for *mono*valent receptors or sites on multivalent receptors and the influence of cell density on these binding characteristics are the major topics of this paper. We consider this a first step in modeling feedback processes within the immune system mediated by antigen-antibody complexes. In employing this approach we isolate the question of how ligands of different valencies compete for binding to cell receptors from considerations concerning the mutually dependent dynamics of cells and ligands.

2 Equilibrium populations of ensembles of ligands

Consider the binding to cell surface receptors of ensembles of ligands of different valence, i.e., of ligands bearing different numbers n of *identical* binding sites. Each ensemble is characterized by a set of positive integers $\mathbf{N} = \{\nu_q, 1 \leq q \leq Q\}$[†] representing the valencies of the Q different ligands (ν_q-mers) in the mixture and their respective total concentrations $X_{\nu_q}, 1 \leq q \leq Q$. For instance, $\mathbf{N} = \{2, 3, 4\}$ means that molecules with valence 2, 3, and 4 constitute the ensemble. A typical example, which we shall use throughout this paper, is that of a set of covalently crosslinked antibody molecules binding to Fc receptors. The above ensemble would then be the set of dimers, trimers and tetramers. Binding experiments of this type have been performed by Dower et al. (Segal et al., 1977; Kagey-Sobotka et al., 1981; Dower et al., 1981; Dembo et al., 1982; Dower et al., 1984; Kent et al., 1994). In this type of system the valence is simply the number of Ig molecules in a covalently crosslinked complex. Hence we shall use the terms ligand of size n to refer to a complex of n Ig molecules. Here n is also the valence. Fc receptors are monovalent and thus the terms receptor and receptor site can be used interchangeably. When we consider binding to immunoglobulin receptors, we shall assume that the two sites on the receptor act independently and have identical binding properties. With this "equivalent site hypothesis" (Perelson and DeLisi, 1980) receptor sites can be treated as monovalent receptors.

We can study the binding of each size molecule in the ensemble separately. The equation for conservation of receptor sites then couples the binding models together.

The concentration of ligands of size n bound to cell-surface receptors at i binding sites ($X_n(i)$) changes according to the following mass-action rate equations (Perelson and DeLisi, 1980; Perelson, 1984). The sequential binding steps in this scheme are illustrated by Fig. 1.

$$\begin{aligned} \dot{X}_n(i) &= (n-i+1)k_i R(0) X_n(i-1) + (i+1)k_{-(i+1)} X_n(i+1) \\ &\quad -[ik_{-i} + (n-i)k_{i+1}R(0)]X_n(i)\ , 1 \leq i \leq n-1\ , \end{aligned} \tag{1}$$

and

$$\dot{X}_n(n) = k_n R(0) X_n(n-1) - nk_{-n} X_n(n)\ . \tag{2}$$

Here $R(0)$ denotes the concentration of free receptor sites and k_i and k_{-i} are the forward and reverse rate constants for the ith binding step, respectively. $X_n(i)$ increases when one of $n-i+1$ free sites of an n-mer bound already at $i-1$ sites binds to a receptor or when one of $i+1$ bound sites on an $X_n(i+1)$ dissociates. Likewise, $X_n(i)$ decreases due to dissociation yielding an $i-1$-fold bound n-mer (third term in Eq. 1) or due to additional binding giving rise to an $i+1$-fold bound n-mer (fourth term in Eq. 1).

Both the total number of receptors R_T and the total number of ligands of size (valence) n, X_{nT}, are conserved. This gives rise to the conservation equations

$$1 = r + \frac{1}{R_T} \sum_{n \in \mathbf{N}} \sum_{i=1}^{n} i X_n(i)\ , \tag{3}$$

and

$$X_{nT} = X_n(0) + \alpha B \sum_{i=1}^{n} X_n(i)\ , \tag{4}$$

[†]Where ν_q is a positive integer.

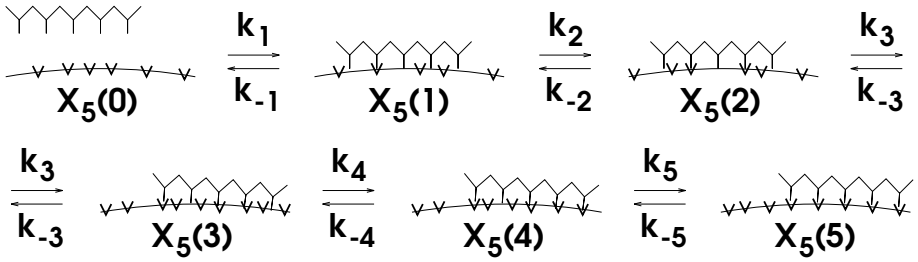

Figure 1: *Free and bound states of a pentamer.* A pentamer, here represented as a complex of 5 immunoglobulin molecules with 5 Fc regions that represent the ligand sites, can form different cell bound states, $X_5(i), i = 1, \ldots, 5$, where i is the number of ligand sites bound to receptors (bold angles on cell surface). In general, each binding step i is governed by its individual forward and reverse rate constant, k_i and k_{-i}, respectively. This same type of binding scheme would govern the interaction of any type of multivalent ligand to monovalent receptors.

for all $n \in \mathbf{N}$. In Eq. 3, $r = R(0)/R_T$ denotes the fraction of free receptor sites. The factor αB in Eq. 4, where B is the number of cells per unit volume, renders the volume concentrations X_{nT} and $X_n(0)$ compatible with the cell surface concentrations $X_n(i), 1 \leq i \leq n$. If volume concentrations are measured in mol/l $\equiv$ M, cell concentrations in 1/ml and surface concentrations in 1/cm^2, then α is the ratio of the mean cell surface area and Avogadro's number times 10^3. Assuming that small B cells are spherical cells with a radius of 3.5 μm, i.e., a surface area of 1.5×10^{-6} cm^2, we obtain $\alpha \approx 2.5 \times 10^{-27}$ cm^2 mol. For monocytes with a radius of 7 μm we obtain $\alpha \approx 10^{-26}$ cm^2 mol and for macrophages with a radius of roughly 30 μm $\alpha \approx 2 \times 10^{-25}$ cm^2 mol. The cell sizes are taken from Miale (1982) and Strand (1978). Please note that the estimated surface areas are derived under the assumption that the cells are spherical. The true surface areas are probably larger, since the overall shape of a cell may resemble an ellipsoid rather than a sphere. Moreover, the surface is usually not smooth but has indentations which implies an even larger surface area. Thus, the surface area and, consequently, the scale factor α may be larger by up to a factor 2 than the estimates we have given. Our results do not depend significantly on the uncertainties due to the actual shape of cells.

Solving Eqs. 1 and 2 at equilibrium yields

$$\overline{X}_n(i) = \binom{n}{i} \left[\prod_{k=1}^{i} K_i R_T \right] \overline{X}_n(0)\, \overline{r}^i \ , \tag{5}$$

for $1 \leq i \leq n$ and all $n \in \mathbf{N}$. We denote equilibrium concentrations by a bar over the variable symbol. The affinities K_i are defined as the ratio k_i/k_{-i}. K_1 is the binding affinity of the ligand from solution to the cell surface and $K_i, i > 1$, is the crosslinking affinity for the $(i-1)$st crosslinking step. For the sake of simplicity, we will assume that all crosslinking affinities have the same value K_x. With this assumption Eq. 5 becomes

$$\overline{X}_n(i) = \binom{n}{i} \frac{K_1 \overline{X}_n(0)}{\kappa_x} R_T \left(\kappa_x \overline{r}\right)^i \ , \tag{6}$$

where we have defined the dimensionless crosslinking affinity $\kappa_x = K_x R_T$.

In order to obtain the equilibrium values $\overline{r}$ and $\overline{X}_n(0)$ we insert Eq. 6 into Eqs. 3 and 4. From the conservation equation for ligand, Eq. 4, we obtain the equilibrium free ligand concentration

$$\overline{X}_n(0) \;=\; \frac{\kappa_x X_{nT}}{\kappa_x + \kappa_1[(\kappa_x\overline{r}+1)^n - 1]} \;, \tag{7}$$

where $\kappa_1 \equiv K_1 \alpha B R_T$ is the dimensionless binding affinity, the counterpart to κ_x. Using expression Eq. 7 we can rewrite the concentration of the bound states in the form

$$\overline{X}_n(i) \;=\; nX_{nT}Q_n(\overline{r})\binom{n}{i}(\kappa_x\overline{r})^i \;, \qquad 1 \le i \le n \;, \tag{8}$$

where

$$Q_n(\overline{r}) \;\equiv\; \frac{K_1 R_T}{n\kappa_x + n\kappa_1[(\kappa_x\overline{r}+1)^n - 1]} \;. \tag{9}$$

Using Eq. 7 we find that the equilibrium fraction of free receptor sites, $\overline{r}$, is given by the solution of

$$\overline{r}\left\{1 + \kappa_x K_1 \sum_{n\in\mathbf{N}} \frac{nX_{nT}(\kappa_x\overline{r}+1)^{n-1}}{\kappa_x + \kappa_1[(\kappa_x\overline{r}+1)^n - 1]}\right\} \;=\; 1 \;. \tag{10}$$

which, in general, must be solved numerically.

The amount of computational effort can be significantly reduced using the excess ligand approximation (Perelson, 1984). Formally, this approximation is equivalent to taking the limit $B \longrightarrow 0$, or $\kappa_1 \longrightarrow 0$. In this limit the conservation equation for ligand, Eq. 4 or Eq. 7 reduces to $X_n(0) = X_{nT}$, i.e., the concentration of free ligand is identical to its total concentration. Moreover, the expression for the fraction of free receptor sites, Eq. 10, then reduces to

$$\overline{r}\left\{1 + K_1 \sum_{n\in\mathbf{N}} nX_{nT}(\kappa_x\overline{r}+1)^{n-1}\right\} \;=\; 1 \;. \tag{11}$$

The excess ligand approximation is valid if the ratio of the concentration of ligand to that of cell-surface receptor sites is much larger than 1. *In vitro* experiments can always be designed to be close to the excess ligand regime, since the cell concentrations can be diluted almost at will. Thus, many theoretical studies of the binding of multivalent ligand have employed the excess ligand approximation (Dembo and Goldstein, 1978; Perelson and DeLisi, 1980; Perelson, 1981; Perelson, 1984; Dower et al., 1984). *In vivo*, however, the ratio of ligand to receptor site concentration can vary from values well below 1 to values much larger than 1. Since we ultimately want to apply our results to *in vivo* situations, we study the influence of the cell density B on the equilibrium binding properties of ligands.

Our model is similar to the models of Gandolfi et al. (1978), Perelson (1981), Vogelstein et al. (1982) and Dower et al. (1984) in that it deals with the binding of *multivalent* ligands to cell surface receptors. It is different, however, in that we shall not impose the excess ligand approximation and we shall allow for *arbitrary* ensembles of ligands of different valencies. The immunon model of Vogelstein et al. (1982) is special in that it assumes that the signal for the cell is provided by a particular receptor-ligand configuration, the immunon. Since, the formation of such an immunon is considered to be *irreversible* it affects the entire binding kinetics.

In the next two sections we will use parameters values valid for the FcγRI[‡] on monocytes. Monocytes have a few tens of thousands of FcγRI (Ravetch and Kinet, 1991) and their expression can be enhanced by as much as 20-fold by interferon-γ (Guyre et al., 1983). The surface area of a monocyte is approximately 6×10^{-6} cm^2, which leads to a FcγRI density of the order of 10^{10} cm^{-2}. The FcγRI has an affinity between 10^8 and 10^9 M^{-1} (van de Winkel and Capel, 1993). To be definite, we use the combination $R_T = 10^{10}$ cm^{-2} corresponding to 2×10^4 receptors per cell and $K_1 = 10^8$ M^{-1}. Dower et al. (1984) find that the non-dimensional crosslinking affinity for the FcγRI on macrophages is of the order of 10. We therefore vary κ_x from 0.1 to 100 with an emphasis on the range 1 to 10. The volume of a monocyte (radius 7 μm) is roughly 10^{-9} ml and, consequently, densely packed monocytes have a concentration of about 10^9/ml. We will investigate cell densities from 10^2/ml to 10^8/ml.

3 Equilibrium binding of a multivalent ligand with valence n

We address two different issues. First, how does the cell density influence the equilibrium binding properties of multivalent ligands and, second, how do ligands of different size compete for binding. We start by studying the binding of a single type of ligand of size (valence) n as the cell density varies. In this way, we isolate the effect of ligand depletion as the cell density increases from the effects due to the competition for binding of ligands of different sizes.

The variables which can be manipulated experimentally are the total ligand concentration, X_{nT}, the cell density, B, and (sometimes) the density of receptors, R_T. An important quantity delineating regimes where binding differs qualitatively is the ratio of the volume concentration of ligand and to that of receptor sites. The volume concentration of ligand sites is given by

$$S \equiv nX_{nT} \tag{12}$$

and that of receptor sites by

$$Y \equiv \alpha B R_T \, . \tag{13}$$

We denote the ratio of ligand site to receptor site concentration by $\Lambda \equiv S/Y$. The volume concentration of receptor sites can be varied by changing the cell concentration B or by changing the number of receptors per cell, $R_T A$, where A is the surface area of the cell. In addition to the regime characterized by an excess of ligand ($\Lambda \gg 1$) we also consider the opposite regime where receptor sites are much more frequent than ligand sites ($\Lambda \ll 1$): the *excess receptor regime*. In what follows we express ligand concentrations in terms of S rather than X_{nT}. This has the advantage of generating results that are independent of n, the valence of the ligand.

3.1 Excess receptor regime

When the concentration of receptor sites is much larger than the concentration of ligand sites, the fraction of free receptor sites is very close to 1. When we consider Eq. 8 for $r = 1$[†], we observe

[‡] FcγRI is the standard abbreviation for the receptor of type I for the Fc portion of immunoglobulin of isotype G.

[†] For the remainder of the paper we omit the overbar denoting the equilibrium value of a variable, since we are interested exclusively in equilibrium quantities in what follows.

that the distribution of bound states, $X_n(i)$, is determined entirely by the crosslinking affinity κ_x and the binomial combinatorial factor (counting the number of ways a particular bound state can be formed). The binding affinity, K_1, and the cell surface receptor density, R_T, only enter as scale parameters in the constant $Q_n(1)$.

$$X_n(i) = SQ_n(1)\binom{n}{i}\kappa_x^i , \qquad 1 \le i \le n \tag{14}$$

$$Q_n(1) = \frac{K_1 R_T}{n\kappa_x + n\kappa_1\left[(\kappa_x+1)^n - 1\right]} = const. \tag{15}$$

If $\kappa_x = 1$, the distribution $X_n(i)$ is symmetrical (binomial) with its maximum at $i_{max} = n/2$. The maximum is shifted towards a greater number of bound sites, when $\kappa_x > 1$, and towards a smaller number of bound sites, when $\kappa_x < 1$. When we increase the ligand concentration S, the concentrations of all bound states increases linearly with S, but their *distribution*, i.e., the relative concentrations, do not change. For small S, the plot on the right for high cell density ($B = 10^7/ml$) in Fig. 2 shows how the concentrations of bound states $X_n(i)$ increase while their (parabolic looking) distribution is preserved. The parabolic part of the surface corresponds to ligand concentrations that are sufficiently small that the system is in the excess receptor regime The linear growth with slope proportional to $Q_n(1)$, which is characteristic of the excess receptor regime, can also be observed in Fig. 3.

Bivalent ligand has been shown to stimulate rat basophilic leukemia cells only poorly whereas its trivalent and larger forms are potent stimulators (Fewtrell and Metzger, 1980). Similarly, T cell-independent stimulation of B cells through their membrane antibodies requires a minimum number of appropriately spaced antigenic determinants on an antigen (Dintzis et al., 1976; Dintzis et al., 1983). A reason for this behavior might be that aggregates of three or more receptors transmit a stimulatory signal much better than those consisting only of two. In general, signal transduction of receptors may require simultaneous crosslinking of a sufficiently large number of receptors, i.e., the formation of bound states with a minimum number of sites bound per ligand. The immunon theory of Dintzis et al. (1976) suggests that this number is of order 10 for B cell activation. From our theory we can calculate the equilibrium number of such potentially stimulating multiply-bound ligands.

The average number of sites bound per ligand (given that it is bound)

$$\langle c \rangle \equiv \frac{\sum_{i=1}^n i X_n(i)}{\sum_{i=1}^n X_n(i)} = \frac{nr\kappa_x(r\kappa_x+1)^{n-1}}{(r\kappa_x+1)^n - 1} \tag{16}$$

is the average number of receptors aggregated by a single ligand (cf. Fig. 4). If the receptors are monovalent, then aggregation can only occur via a single ligand and $\langle c \rangle$ is thus the average cluster size. If receptors are multivalent, then a single receptor can bind multiple ligands and larger clusters can form.

In addition to the average number of sites bound per ligand we can also compute higher moments of the distribution. The second moment

$$\langle c^2 \rangle \equiv \frac{\sum_{i=1}^n i^2 X_n(i)}{\sum_{i=1}^n X_n(i)} = \frac{nr\kappa_x\left(r\kappa_x+n\right)\left(r\kappa_x+1\right)^{n-2}}{(r\kappa_x+1)^n - 1} \tag{17}$$

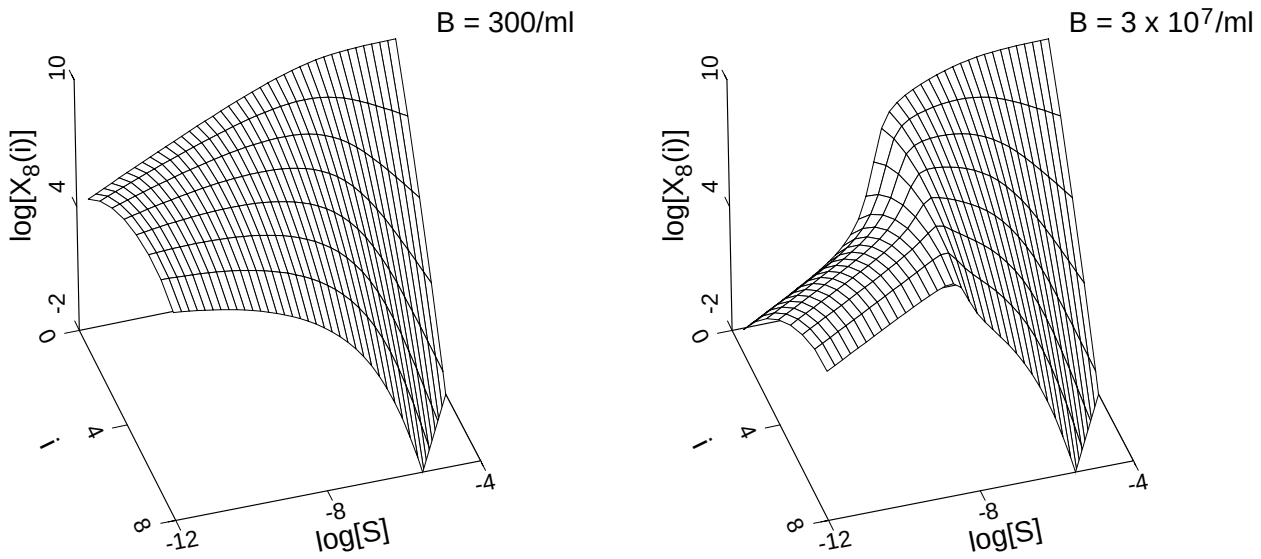

Figure 2: *Distribution of bound states.* We show the concentration of octomers ($n = 8$) bound at i sites as a function of the total concentration of ligand sites S, where S is in molar units and $X_8(i)$ is expressed in molecules/cm^2. When S is larger than the concentration of receptor sites Y ($B = 300/ml \iff Y = 3 \times 10^{-15}$ M) over the entire range of ligand concentrations no effect of ligand depletion can be noticed. As the cell density is increased ligand depletion occurs and reduces the concentration of the cell bound states obtained for ligand concentrations that are smaller than the receptor concentration. In the excess receptor regime ($S \ll Y$) ligands bind at the maximum number of sites allowed by the crosslinking affinity κ_x and the ligand valence n. The bound states $X_8(i)$ switch back to the excess ligand distribution approximately where $S = Y$, i.e., at $S \approx Y = 3 \times 10^{-10}$ M for $B = 3 \times 10^7$/ml. The other parameters are $K_1 = 10^8$ M^{-1}, $R_T = 10^{10}$ cm^{-2}, $\kappa_x = 10$ and $\alpha = 10^{-26}$ cm^2 mol.

and hence the variance

$$\sigma_c^2 \equiv \langle c^2 \rangle - \langle c \rangle^2 = \frac{n r \kappa_x \left[r\kappa_x + n - 1 - (r\kappa_x + n)(r\kappa_x + 1)^{-n} \right]}{(r\kappa_x + 1)^2 \left[1 - (r\kappa_x + 1)^{-n} \right]} . \tag{18}$$

In the excess receptor regime the average number of sites bound per ligand is given by

$$\langle c \rangle_{er} = \frac{n\kappa_x(\kappa_x + 1)^{n-1}}{(\kappa_x + 1)^n - 1} \approx n \frac{\kappa_x}{\kappa_x + 1} , \tag{19}$$

where the approximate expression is valid for sufficiently large n. The average number of sites bound per ligand is maximal in the excess receptor regime, $\langle c \rangle_{er} \geq \langle c \rangle$, since the derivative of $\langle c \rangle$ is

$$\frac{\partial \langle c \rangle}{\partial r} = \frac{n\kappa_x(\kappa_x r + 1)^{n-1}}{\left[(\kappa_x r + 1)^n - 1\right]^2} \sum_{i=2}^{n} \binom{n}{i} (\kappa_x r)^i > 0 \tag{20}$$

for $n > 1$ and all r. For monomers, $n = 1$, and as is to be expected, $\langle c \rangle$ is 1 for all r.

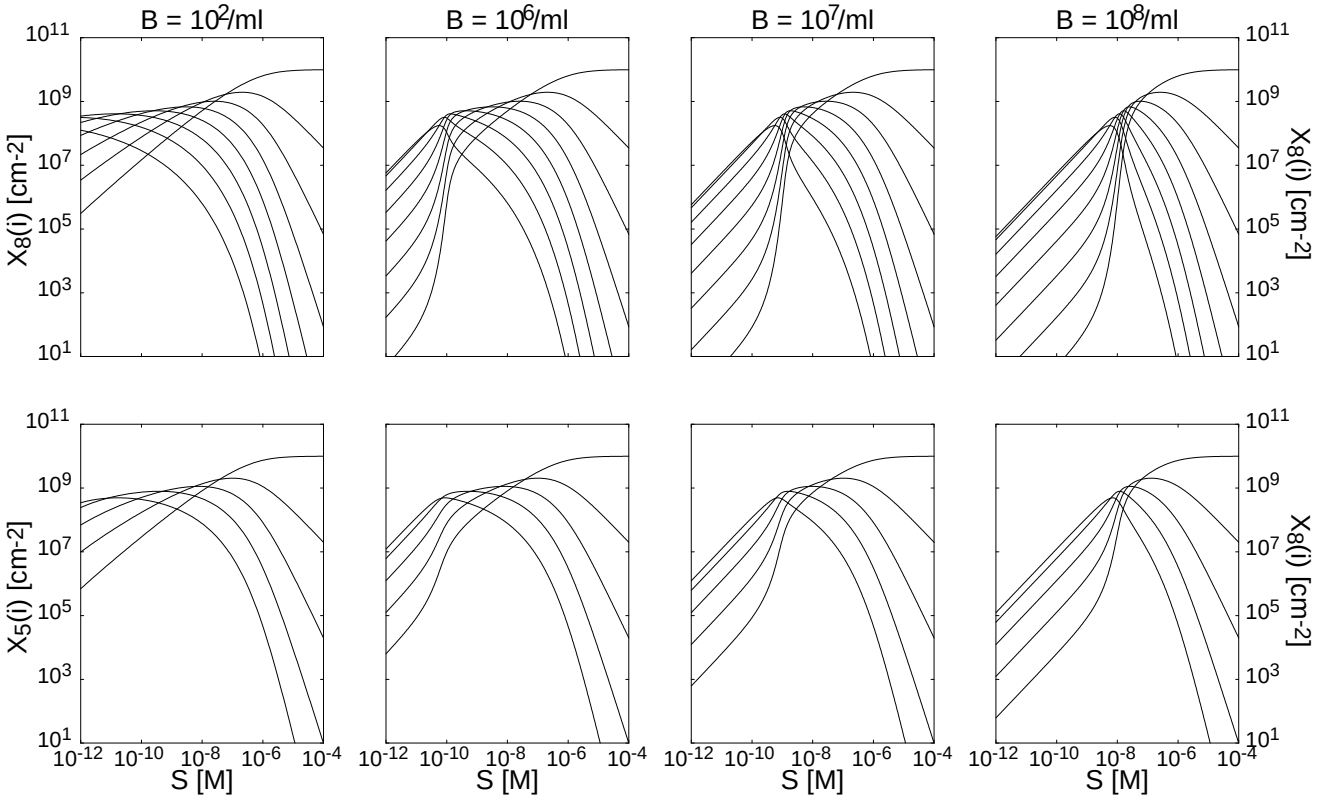

Figure 3: *Concentration of bound states.* The concentrations of the different bound states, $X_n(i)$, for an octomer ($n = 8$, top row) and a pentamer ($n = 5$, bottom row) at different cell densities ($B = 10^2$/ml, 10^6/ml, 10^7/ml, and 10^8/ml). In each panel the set of curves show the ligand concentration, $X_n(i)$ for $i = 1, ..., n$. At the right axis, $S = 10^{-5}$ M, the curves are ordered with $i = 1$ at the top and $i = n$ at the bottom. Increasing the receptor concentration by increasing B diminishes the number of ligands bound at any given ligand concentration. This is particularly evident at low ligand concentrations, e.g. $S = 10^{-13}$ M. Moreover, the transition range from the excess receptor to the excess ligand regime moves to the right with B. Parameters are as in Fig. 2.

Additional information can be obtained from the fraction of ligands bound at more than m sites

$$b(m) \;=\; \frac{\sum_{i=m+1}^{n} X_n(i)}{\sum_{i=1}^{n} X_n(i)} \;, \tag{21}$$

which in the excess receptor regime evaluates to

$$b_{er}(m) \;=\; 1 \;-\; \frac{(\kappa_x + 1)^m - 1}{(\kappa_x + 1)^n - 1} \;. \tag{22}$$

The fraction of bound states with more than m sites bound per ligand, $b_{er}(m)$, increases with both the length of the oligomer n and the crosslinking affinity κ_x.

In summary, when there is an excess of receptors, ligands bind with the maximum number of sites allowed by the binding characteristics, i.e., the crosslinking affinity κ_x and the ligand size (valence) n. However, the number of bound ligands per cell is reduced relative to that for the same total ligand concentration at low cell density. Figures 2 and 3 as well as the Scatchard plots in Fig. 5 show a dramatic reduction in the concentration of bound ligands when the cell density

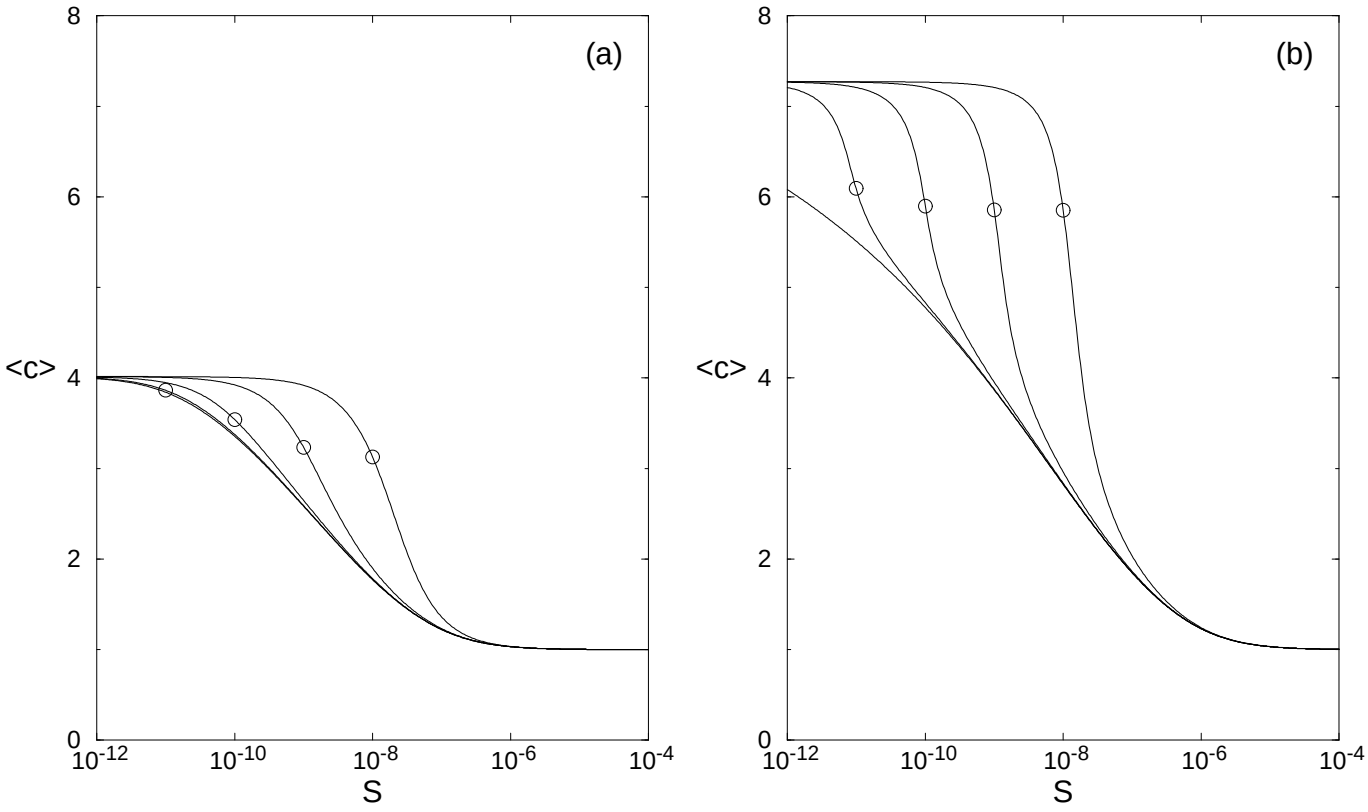

Figure 4: *Average number of sites bound per ligand.* For an octomer ($n = 8$) we show $\langle c \rangle$ for different cell densities. The circle denotes the point $\Lambda = 1$ where the ligand concentration is identical to the receptor concentration on the respective curve. (a) $\kappa_x = 1$, (b) $\kappa_x = 10$. The curves in both (a) and (b), from left to right, are for cell densities $B = 10^2$/ml, 10^5/ml, 10^6/ml, 10^7/ml, and 10^8/ml, respectively. When $B = 10^2$/ml the system is in the excess ligand regime for the entire range of ligand concentration S (cf. Fig. 2). K_1, R_T, and α have the same values as in Fig. 2.

B increases. The concentration of bound ligands is reduced, because free ligand is depleted significantly. Equation 7 shows that the concentration of free ligand is inversely proportional to the cell density when the cell density is sufficiently large.

3.2 Excess ligand regime

In the excess ligand approximation the fraction of free receptor sites, r, can be determined by Eq. 11. For a single ligand Eq. 11 simplifies to

$$1 \;=\; r\left[1 + K_1 S\left(\kappa_x r + 1\right)^{n-1}\right] \;. \tag{23}$$

This equation has a single real solution, r, with $0 < r < 1$. To see this notice that $r = 0$ can not be a solution, and that for $r > 0$ the polynomial $1 + K_1 S\left(\kappa_x r + 1\right)^{n-1}$ is larger than 1 and increases monotonically. Consequently, it has a single intersection with the monotonically decreasing function $1/r$ at a value of $r < 1$.

For small ligand concentrations ($S \longrightarrow 0$, keeping $Y \ll S$ since we are in the excess ligand regime) the fraction of free receptor sites, r, approaches 1 and the bound states are distributed as in the excess receptor regime. As the ligand concentration increases, bound states with few

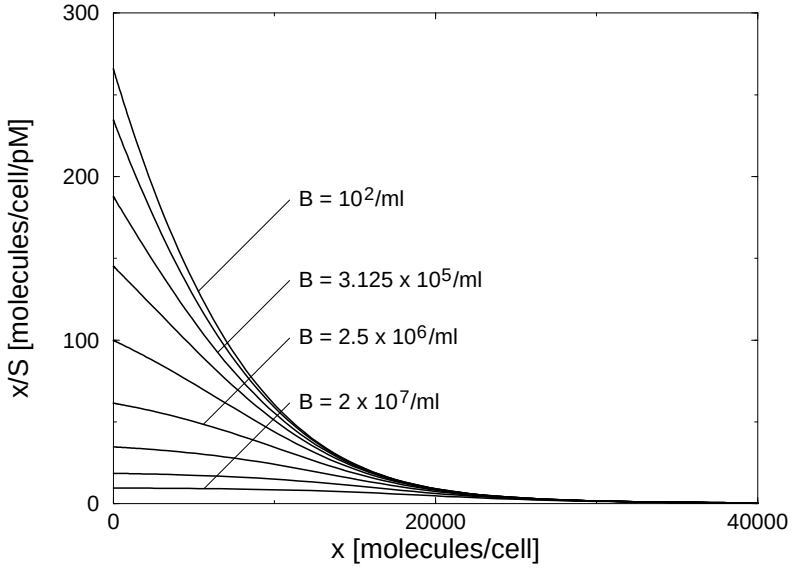

Figure 5: *Binding of trimers ($n = 3$) at different cell densities.* Binding is represented as a Scatchard plot. The different curves are for cell densities $B = 10^2$/ml, 10^5/ml, 3.125×10^5/ml, 6.25×10^5/ml, 1.25×10^6/ml, 2.5×10^6/ml, 5×10^6/ml, 10^7/ml, and 2×10^7/ml (from top to bottom). The variable $x \equiv \sum_{i=1}^{n} X_n(i)$ denotes the concentration of bound ligand. With increasing cell density the low ligand concentration part of the Scatchard plot drops indicating a decrease of cell bound ligand. K_1, R_T, κ_x, and α are chosen as in Fig. 2.

sites bound are favored relative to those with many sites bound (see Fig. 4). For large S, almost every receptor is bound. However, no crosslinks are established, since each ligand is bound at a single site. In Fig. 4a this occurs for $S \approx 10^{-7}$ (there $\langle c \rangle$ approaches 1), and at slightly larger ligand concentrations in Fig. 4b. We observe the same phenomenon in Figs. 2 and 3 (for $B = 10^2/\mathrm{ml}$) since the concentration of singly bound ligand $X_n(1)$ increases monotonically with S and eventually saturates at $X_n(1) = R_T$. The concentrations of all multiply bound ligands $X_n(i), 1 < i \leq n$, go through a maximum as S is varied. The ligand concentration where this maximum occurs decreases with i, the number of sites bound. For the octomer in Fig. 2 ($B = 10^2/ml$) we find the maximum of doubly bound ligand $X_8(2)$ at $S \approx 3.5 \times 10^{-8}$M, for $X_8(3)$ at $S \approx 2 \times 10^{-9}$M, for $X_8(4)$ at $S \approx 3 \times 10^{-10}$M, for $X_8(5)$ at $S \approx 3 \times 10^{-11}$M, and for $X_8(6)$ at $S \approx 2 \times 10^{-12}$M. The concentrations of 7-fold and 8-fold bound ligand attain their maximum below 10^{-13}M, i.e., outside the range of ligand concentrations we show in Fig. 2.

We conclude, that in the excess ligand regime the concentration of bound ligand is maximized. At low ligand concentration maximizing the number of bound ligands does not conflict with binding the ligand at as many sites as possible. At large ligand concentration, however, the distribution of cell bound states $X_n(i)$ changes such as to accommodate the maximum possible number of ligands on the cell surface thus reducing the number of sites bound per ligand.

3.3 Transition from the excess receptor to the excess ligand regime

There is a fairly sharp transition in the average number of ligand sites bound, $\langle c \rangle$, as the ligand concentration is varied from the excess receptor to the excess ligand regime. This transition

is centered approximately at $S = Y$, i.e., where the concentration of receptors is equal to the concentration of binding sites on the ligand (marked by open circles in Fig. 4). The cell density at which ligand depletion due to an excess of receptors becomes significant decreases as the crosslinking affinity κ_x increases. We witness this transition from the excess receptor to the excess ligand regime also in the concentrations of cell bound states $X_n(i)$ in Figs. 2 and 3. Furthermore, Fig. 4 shows that the transition is completed within an order of magnitude of the ligand concentration at which $S = Y$. For FcγRI on monocytes the cell density must be at least 10^6/ml, if $\kappa_x = 1$ to see any deviation from the excess ligand regime behavior (Fig. 4a). However, the effects of ligand depletion can be noticed at cell densities of 10^4/ml or above for ligand site concentrations below 10^{-8} M, if $\kappa_x = 10$ (Fig. 4b). Typical cell densities in *in vitro* experiments are 10^5/ml to 10^6/ml. In contrast, *in vivo* monocyte densities up to 10^8/ml are possible in environments where the cells are densely packed. Thus ligand depletion effects should be observable for monocytes *in vitro* and possibly play a role *in vivo*. This can also be true for other cell types. Later, in section 5, we shall discuss the effects of ligand depletion on B cell activation by T-independent antigens.

In general, the range of ligand concentrations where the transition occurs from binding multiple sites to a single site per ligand determines whether cell density effects are significant. This transition range is centered at $S = K_1^{-1}$. If S is much smaller than this then binding is an extremely rare event. When S is larger than this multiple sites bind unless the ligand concentration exceeds the receptor concentration significantly. Therefore, we expect to find ligand depletion for cell densities of the order of $B_d = 1/(\alpha R_T K_1)$, the cell density which makes the receptor concentration $Y = K_1^{-1}$. For FcγRI on monocytes this crude estimate yields $B_d \approx 3 \times 10^7$/ml, for Fc$\gamma$RI on macrophages $B_d \approx 2 \times 10^6$/ml, for Fc$\gamma$RII on B cells $B_d \approx 10^{11}$/ml. Comparing B_d for monocytes with Fig. 4 we see that we over-estimate the necessary cell density by at least 2 orders of magnitude which is due to the fact that the transition from binding the maximum number of sites to a single site per ligand typically takes place for ligand concentrations extending over several orders of magnitude (e.g., the transition extends over ligand concentrations $10^{-13} < S < 10^{-7}$ for the octomers in Fig. 4). Assuming that the same holds true for Fc receptors on macrophages and B cells we conclude that cell density effects may in fact occur for the binding of immune complexes to macrophages. For FcγRII on B cells, however, the necessary cell density is still of the order of 10^9/ml, a concentration which can be achieved only if the cells are packed at maximum density. Binding to the immunoglobulin receptor on B cells, however, may show receptor density effects as we shall discuss in section 5. As κ_x increases the cell concentration where ligand depletion becomes important decreases, since the transition range becomes wider.

4 Equilibrium binding of heterogeneous ligand ensembles

In the previous section we discussed the binding of ligands of uniform size (valence) n to cell surface receptors. When ligands are formed *in vivo* by aggregation of smaller subunits as, for instance, antibody-antigen complexes, the resulting aggregates can be of different sizes. We are interested in determining, at equilibrium, the distribution of bound ligand states for *heterogeneous* ensembles or mixtures of ligands of different size and valence. Because the formation of antigen-antibody complexes is a reversible process aggregates may change their size. Thus, when

analyzing the binding of antigen-antibody complexes to Fc receptor-bearing cells one needs to simultaneously solve for the equilibrium distribution of aggregates in solution and on the surface. Here, as a first problem, we wish to bypass the computation of the distribution of aggregates in solution. Thus, we study the binding of ligand ensembles with a *fixed* total concentration for each size ligand. This, for example, would apply to covalently cross-linked antibody aggregates.

We consider ensembles where the n-mers[†] are distributed according to

$$X_{nT} = X g^{n-1}, \qquad 1 \le n \le N, \qquad 0 < g < 1 \; . \tag{24}$$

Note that $X = X_{1T}$ is the total monomer concentration. The *ensemble weight* g determines how the frequency of ligands in the ensemble decreases as their size increases. A distribution of this form arises when bivalent antibodies bind bivalent antigen in the absence of cell-bound receptors (Goldberg, 1952; DeLisi and Perelson, 1976; Perelson and DeLisi, 1980). In this case, the value of g depends on the total concentrations of antibody and antigen and their mutual affinity. For fixed antibody concentration, g decreases monotonically as the antigen concentration increases. On the other hand, it increases monotonically with increasing antibody concentration, when the antigen concentration is fixed. $g = 0.25$ at low antigen concentration when the antibody concentration is equal to the inverse of the affinity. When the antibody concentration is much larger than the inverse of the affinity, g approaches 1 for small antigen concentration. When the antigen and antibody concentrations are identical g is roughly half of its value at low antigen concentration. g approaches 0 when the antigen concentration becomes much larger than the antibody concentration. For the distribution Eq. 24, the total concentration of binding sites is

$$S = \sum_{n=1}^{N} n X_{nT} = X \, \frac{1 - [1 + (1-g)N] g^N}{(1-g)^2}. \tag{25}$$

Since ligands of different size compete for binding, the distribution of bound states for the heterogeneous ensemble is not simply the superposition of the distributions of bound states for the individual n-mers in the ensemble. In Fig. 6 we show for the excess ligand regime, i.e. very low cell density, the number of sites bound per ligand, given the ligand is bound, averaged over the entire ensemble

$$\langle c \rangle \;\equiv\; \frac{\sum_{n=1}^{N} \sum_{i=1}^{n} i X_n(i)}{\sum_{n=1}^{N} \sum_{i=1}^{n} X_n(i)} \; , \tag{26}$$

and the average number of sites bound for individual bound n-mers in the ensemble

$$\langle c_n \rangle \;\equiv\; \frac{\sum_{i=1}^{n} i X_n(i)}{\sum_{i=1}^{n} X_n(i)} \; . \tag{27}$$

For sufficiently low ligand concentrations the average over any particular n-mer in the heterogeneous ensemble, $\langle c_n \rangle$, takes the same value as in a homogeneous ensemble of the same n-mer. Obviously, an n-mer binds independently from all other ligands in the ensemble provided the ligand concentration is so low that ligands do not compete for receptors. We find this independence from the ensemble context of the n-mer average $\langle c_n \rangle$ at low ligand concentration irrespective of the composition of the ensemble. Thus, for small S the n-mer averages approach the same value whether the ligand concentration within the ensemble decreases slowly or rapidly with n (Compare Fig. 6a for $g = 0.5$ with Fig. 6b for $g = 0.1$). Further, as $S \longrightarrow 0$, receptors must be in excess and thus the n-mer average approaches the value given by Eq. 19.

[†]We consistently use the term n-mers for ligands of a particular size while we employ the term ligands for a heterogeneous set of *different* n-mers

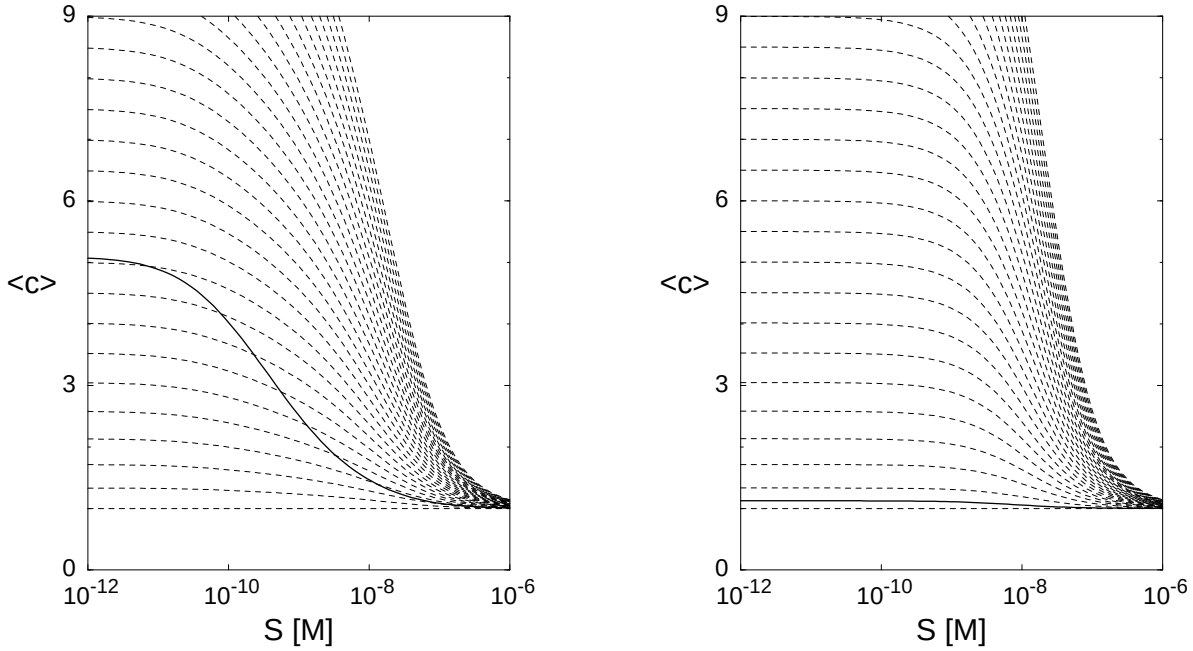

Figure 6: *Influence of the total concentration of ligands on the average number of sites bound.* The total concentration of ligand sites S is given by Eq. 25. The solid line is $\langle c \rangle$, the average number of bound sites, where the average is taken over the bound states of the entire ensemble of ligands ($1 \leq n \leq 256$). The dashed lines show $\langle c_n \rangle$, the average number of sites bound per n-mer given that the n-mer is bound, for $n = 1, \ldots, 29$, with $n = 1$ the lower curve and $n = 29$ the upper curve. (a) $g = 0.5$, an ensemble with a fairly high proportion of large ligands. (b) $g = 0.1$, an ensemble having a moderate proportion of large ligands. Both plots are for relatively weak crosslinking ($\kappa_x = 1$) in the excess ligand regime ($B = 10^2$/ml). The affinity, receptor density, and α, have the same values as in Fig. 2, i.e., $K_1 = 10^8$ M^{-1}, $R_T = 10^{10}$ cm^{-2} and $\alpha = 10^{-26}$ cm^2 mol.

Whereas $\langle c_n \rangle$ becomes independent of g for small S, the ensemble average $\langle c \rangle$ depends upon g for all values of S. The faster the fraction of n-mers in the ensemble decreases with their size n, i.e., the smaller g, the smaller is the average number of sites bound per ligand. As g decreases the bound states involve predominantly small ligands due to their dominance in the ensemble. However, the ensemble average $\langle c \rangle$ is larger than the superposition of the n-mer averages $\langle c_n \rangle$ weighted by the frequency of the corresponding n-mer in the ensemble g^{n-1} indicating a preferential binding of larger ligands. In fact, the fraction of n-mer bound to receptors, given by

$$\frac{\alpha B \sum_{i=1}^{n} X_n(i)}{X_{nT}} \;=\; \frac{\kappa_1 \left[(\kappa_x r + 1)^n - 1\right]}{\kappa_x + \kappa_1 \left[(\kappa_x r + 1)^n - 1\right]} \;, \tag{28}$$

increases monotonically with n for all r.

We cannot calculate exactly the ensemble average of bound ligand sites in the excess receptor regime, $\langle c \rangle_{er}$. However, we are able to approximate $\langle c \rangle_{er}$, with high accuracy, when g is not too large, e.g. $g < 0.8$. First, observe that in the ensemble free ligands are hardly depleted, if they are small, and significantly depleted, if they are large (cf. Fig. 7). In the excess receptor regime ($r = 1$) the concentration of free ligands $X_n(0)$ is given by (cf. Eq. 7)

$$X_n(0) \;=\; X_{nT} \left\{ 1 + \frac{\kappa_1}{\kappa_x} \left[(\kappa_x + 1)^n - 1 \right] \right\}^{-1} \;. \tag{29}$$

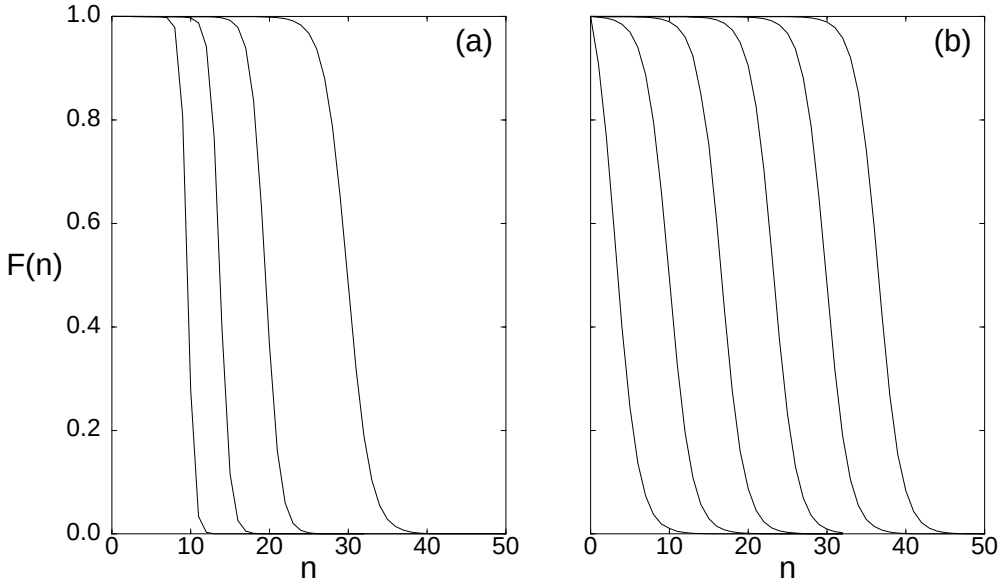

Figure 7: *Fraction of unbound n-mers.* (a) $\kappa_1 = 10^{-9}$ and $\kappa_x = 1, 2, 4, 10$, from right to left. (b) $\kappa_x = 1$ and $\kappa_1 = (10^{-11}, 10^{-9}, 10^{-7}, 10^{-5}, 10^{-3}, 10^{-1}$, from right to left. Notice in (a) that most of the small n-mers are unbound, whereas most of the large n-mers are bound. The characteristic value n_c where half of the n-mers are bound depends upon κ_x and κ_1. (a) shows that n_c decreases with κ_x and (b) shows that n_c decreases with κ_1. Furthermore, we see in (a) that the slope at the transition increases with κ_x.

For small n the first term in curly brackets dominates, whereas for large n the second term dominates. The second term in the curly brackets is greater than 1 for

$$n \; > \; n_c \; = \; \frac{\log(1 + \kappa_x/\kappa_1)}{\log(1 + \kappa_x)} \; , \tag{30}$$

where $\kappa_1 = K_1 \alpha BR = K_1 Y$. As a function of n the transition from no depletion to large depletion is relatively sharp. The slope of the fraction of unbound ligand $X_n(0)/X_{nT}$ at the transition increases with the crosslinking affinity κ_x (Fig. 7a). We can thus approximate the concentration of free ligand by

$$X_n(0) \; = \; \begin{cases} X_{nT} \; , & \text{for} \quad n \leq n_c \\ X_{nT} \, \dfrac{\kappa_x}{\kappa_1 \left[(\kappa_x + 1)^n - 1 \right]} \; , & \text{otherwise.} \end{cases} \tag{31}$$

which over-estimates the concentration of free ligand. The accuracy increases with increasing κ_x, since the slope of $X_n(0)/X_{nT}$ at the transition increases.

Using the approximate values, Eq. 31, for unbound ligands $X_n(0)$ and another approximation assuming $g \ll \kappa_x + 1$ (cf. Appendix; Eq. A15), we obtain for the average number of receptors bound per ligand in the excess receptor regime

$$\langle c \rangle_{er} \; \approx \; \kappa_x \, \frac{\frac{1 - \{1 + [1 - g(\kappa_x + 1)] n_c\} \{g(\kappa_x + 1)\}^{n_c}}{[1 - g(\kappa_x + 1)]^2} + \frac{\kappa_x g^{n_c}}{\kappa_1 (\kappa_x + 1)} \left\{ \frac{1 + (1 - g) n_c}{(1 - g)^2} + \frac{n_c + 1}{(\kappa_x + 1)^{n_c + 1} - 1} \right\}}{(\kappa_x + 1) \frac{1 - [g(\kappa_x + 1)]^{n_c}}{1 - g(\kappa_x + 1)} + \left[\left(\frac{\kappa_x}{\kappa_1} + 1 \right) g^{n_c} - 1 \right] \frac{1}{1 - g}} \; . \tag{32}$$

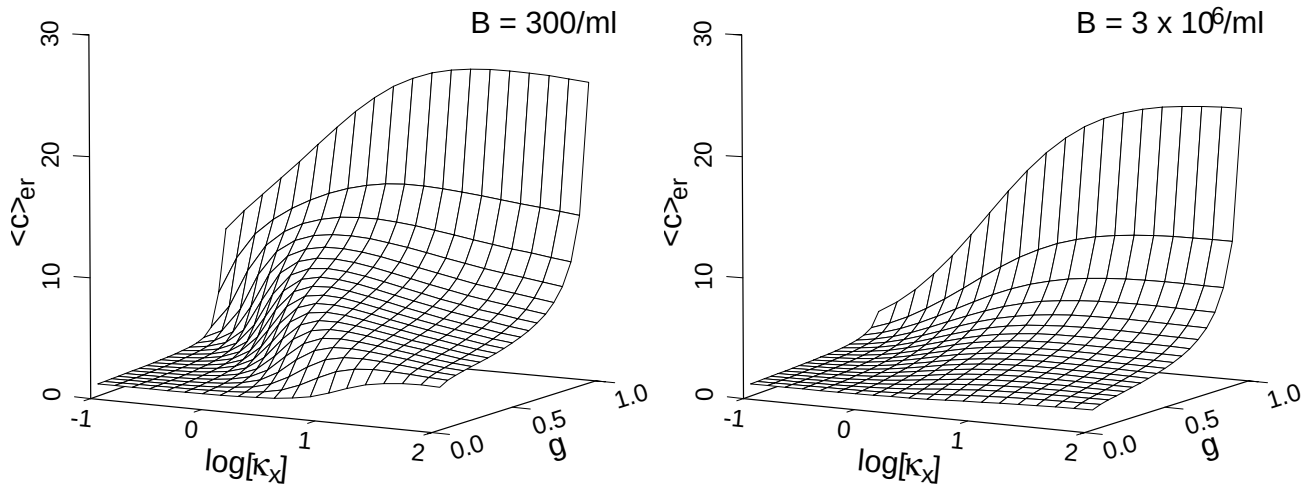

Figure 8: $\langle c \rangle_{er}$ *in the excess receptor regime as a function of* κ_x *and* g. For cell densities $B = 300/\mathrm{ml}$ (left) and $B = 3 \times 10^6/\mathrm{ml}$ (right) we show the average number of sites bound per ligand in the excess receptor regime $\langle c \rangle_{er}$ versus the crosslinking affinity κ_x and the ensemble weight g. For fixed g, $\langle c \rangle_{er}$ has a unique maximum as function of κ_x. $\langle c \rangle_{er}$ increases monotonically with g for fixed κ_x. The ligand concentration is chosen small enough to be always in the excess receptor regime ($S = 10^{-20}$ M suffices for all purposes). The other parameters are $K_1 = 10^8$ M^{-1}, $R_T = 10^{10}$ cm^{-2}, and $\alpha = 10^{-26}$ cm^2 mol.

If $n_c \gg 1$ and $g(\kappa_x + 1) < 1$ this expression reduces to

$$\langle c \rangle_{er} \approx \frac{1-g}{1-g(\kappa_x+1)} . \tag{33}$$

Both results are in good agreement with the numerical solution of the exact Eqs. 3, 4, and 6 shown in Figs. 8 and 9. The relative error is less than 5% for $g < 0.8$; for $g > 0.8$ and $\kappa_x < 1.0$ the error due to neglecting g with respect to $(\kappa_x + 1)^k$, $k \geq 1$, in the step from Eq. A14 to A15 increases the total relative to values up to 50%.

For sufficiently large ensemble weight g we observe a crosslinking affinity κ_x which maximizes $\langle c \rangle_{er}$ (cf. Fig. 8). The reason is that for given g, κ_1, and $r = 1$, both the concentration of bound n-mer molecules and of bound n-mer sites attains a maximum at an intermediate κ_x. Moreover, $\langle c \rangle_{er}$ increases monotonically with g and decreases monotonically with B (cf. Fig. 9). When the cell density decreases, $\langle c \rangle_{er}$ either reaches a plateau, if $g(\kappa_x + 1) < 1$, or increases indefinitely, otherwise. It appears that large ligands have a competitive advantage when receptors become scarce, provided the increase in their capacity to bind at multiple sites outweights the effect of their decreasing frequency in the ensemble.

When the ligand concentration increases we observe two qualitative different types of behavior. For sufficiently small crosslinking affinity κ_x and ensemble weight g both the ensemble average $\langle c \rangle$ and the n-mer averages $\langle c_n \rangle$ decrease monotonically approaching 1 for large S (see Fig. 6). The ligand concentration where the averages start to decrease is determined by the ensemble composition. The greater the fraction of large ligands the smaller the value of S where

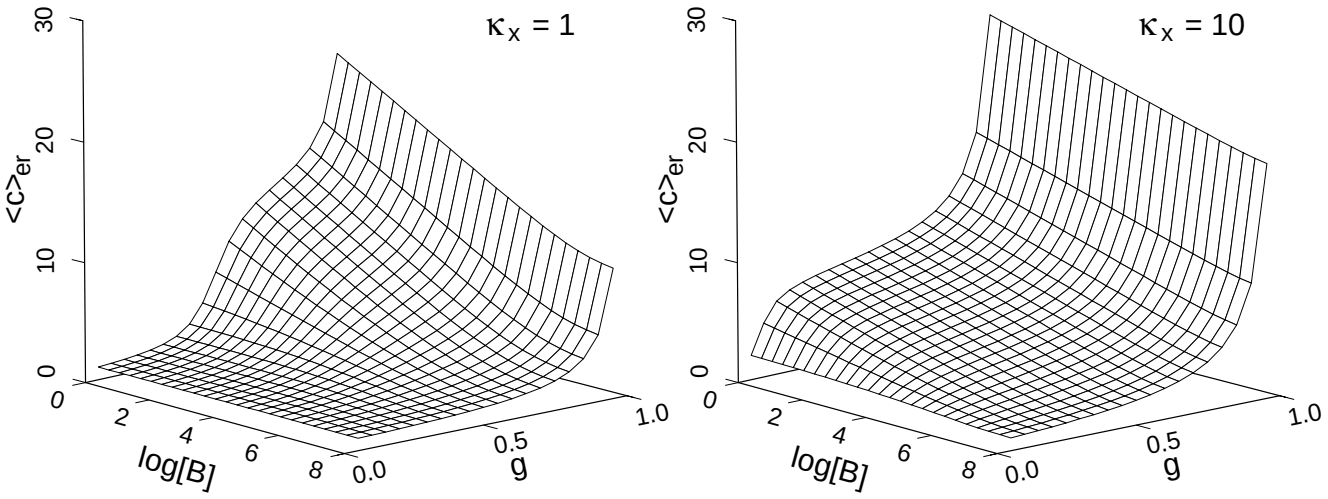

Figure 9: $\langle c \rangle_{er}$ *in the excess receptor regime as function of* B *and* g. For crosslinking affinities $\kappa_x = 1$ (left) and $\kappa_x = 10$ (right) we plot the average number of sites bound per ligand in the excess receptor regime $\langle c \rangle_{er}$ versus the cell density B and the ensemble weight g. $\langle c \rangle_{er}$ decreases monotonically with B for fixed g and increases monotonically with g for fixed B. As B decreases, $\langle c \rangle_{er}$ either reaches a plateau, in the case $g(\kappa_x + 1) < 1$ (i.e., for $g < 0.5$ in the left plot), or increases indefinitely otherwise. The parameters are $K_1 = 10^8$ M^{-1}, $R_T = 10^{10}$ cm^{-2}, and $\alpha = 10^{-26}$, cm^2 mol.

the averages start to decrease (compare Figs. 6a and 6b). Moreover, the ensemble average $\langle c \rangle$ decreases significantly faster than the n-mer averages $\langle c_n \rangle$ (Fig. 6a). The preference for binding large ligands is diminished as the ligands are beginning to compete for free receptor sites.

On the other hand, when κ_x and g are sufficiently large the ensemble average $\langle c \rangle$ first increases with S, attains a maximum, and finally decreases to 1 for $S > K_1^{-1}$ (see Fig. 10). The n-mer averages, however, still decrease monotonically. The ensemble average of sites bound per ligand has a maximum, because in the intermediate regime of ligand concentrations, where crosslinks are still frequent but ligands begin to compete for receptor sites, large ligands have a competitive advantage over small ones. This advantage increases with the crosslinking affinity κ_x and with the ensemble weight g. Consequently, the maximum of $\langle c \rangle$ increases with g and κ_x. The difference between the maximum and the excess receptor limit of $\langle c \rangle$ is largest for g between 0.75 and 0.8 and increases monotonically with κ_x for fixed g. Finally, both the relative and the absolute size of the maximum increase with decreasing cell density B.

5 Discussion

We have analyzed the equilibrium binding properties of multivalent ligands and heterogeneous ensembles of ligands of different valencies to cell surface receptors. We have shown that in both cases the volume concentration of receptors (number of receptors/cell $\times$ cell density) has a pronounced effect on the total amount of ligand bound and on the total number of sites bound

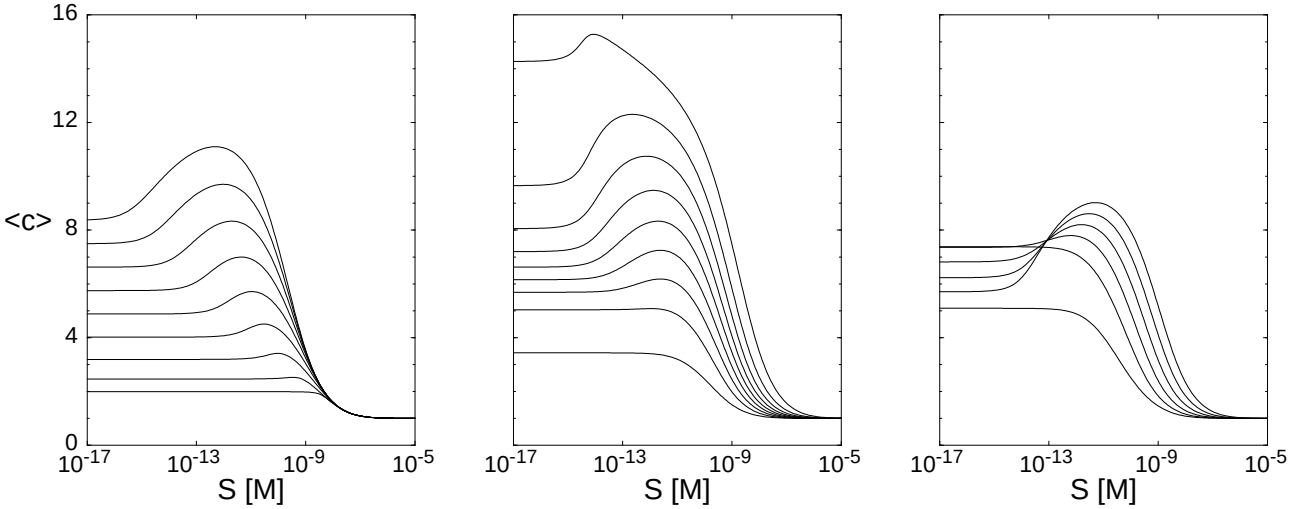

Figure 10: *Ensemble average of the number of sites bound.* We show $\langle c \rangle$, the ensemble average of the number of sites bound per ligand. Provided the ensemble weight g and the crosslinking affinity κ_x are large enough, $\langle c \rangle$ has a maximum for intermediate ligand concentrations. (a) shows the dependence of $\langle c \rangle$ upon the cell density B (from 1/ml to 10^8/ml in factors of 10, from top to bottom) for $g = 0.5$ and $\kappa_x = 10$. (b) shows its dependence upon g (from 0.1 to 0.9 in steps of 0.1, from bottom to top) for $B = 100$/ml and $\kappa_x = 10$. (c) shows its dependence upon κ_x (from 1 to 32 in factors of 2, from bottom to top at high ligand concentration) for $B = 100$/ml and $g = 0.5$. Furthermore, $K_1 = 10^9$ M^{-1} and $R_T = 10^9$ cm^{-2}.

per ligand.

We first discuss the case of a single multivalent ligand. Equilibrium binding differs qualitatively according to whether the receptor concentration is much larger than the ligand concentration or much less. In the first case, the excess receptor regime, the ligands bind with as many sites as possible (which depends predominantly upon the crosslinking affinity). However, the number of bound ligands per cell is smaller in the excess receptor regime than in the excess ligand regime, where ligands are much more frequent than receptors. Due to the reversibility of the binding not every ligand binds with all its sites in the excess receptor regime. There is still a distribution of cell-bound ligand states, bound states for short, which differ by the number of sites bound per ligand. In the excess receptor regime the concentrations of all bound states increases linearly with the ligand concentration while their relative concentrations remain the same.

Close to the point where receptor and ligand concentrations are identical there is a fairly sharp transition from behavior characteristic of the excess receptor regime to behavior characteristic of the excess ligand regime. When the ligand concentration exceeds the receptor concentration by one order of magnitude all binding characteristics are almost indistinguishable from the excess ligand regime. Now, in distinction to the excess receptor regime, the number of ligands bound per cell is maximized at the expense of the number of sites bound per ligand. For large ligand concentrations almost every ligand is bound at only one site. The concentration of singly bound ligand increases monotonically with the ligand concentration and finally saturates at the value of the total receptor concentration. The concentrations of the multiply bound states, i.e., the crosslinked states, attain a maximum for some intermediate ligand concentration and approach

zero for high and low ligand concentrations. The larger the number of sites bound the smaller is the ligand concentration for which the corresponding bound state attains its maximum. Thus, we re-establish the sigmoid binding curve for singly bound states and the bell-shaped binding curves for crosslinked states that have been discussed extensively in the literature (DeLisi and Perelson, 1976; Perelson and DeLisi, 1980; Vogelstein et al., 1982; Perelson, 1984; Dower et al., 1984).

Our theory should have many applications in cell biology and immunology. Here we give a single example. Using our theory to reinterpret data published by Dintzis et al. (1983) we argue that receptor density effects can be observed in the T-independent response of B cells to multivalent molecules studied *in vitro*. A characteristic of reaching the excess receptor regime is a relatively steep slope of the rising part of the "bell-shaped" crosslinking function. The rising part of the crosslinking curve occurs at low ligand concentrations and thus the shape of the curve is strongly influenced by the receptor density. If the multivalent ligands were in excess of receptors, then the crosslinking function would rise very slowly. However, in the response functions measured by Dintzis et al. (1983) the curves rise rapidly. This qualitative feature can be noticed in each of the response curves in the experiments of Dintzis et al. (1983) and we reproduce it in Fig. 11.

Figure 11 shows, F, the fraction of surface immunoglobulin receptor sites in cell-bound states containing more than 10 ligand sites, predicted by our theory for the types of ligands studied by Dintzis et al. (1983). Assuming that the B cell response is proportional to F we obtain good agreement with Dintzis' data, when we choose $K_1 = 10^5$ M^{-1}, $\kappa_x = 1$, $\alpha = 2.5 \times 10^{-27}$ cm^2 mol (see section 2), $R_T = 4 \times 10^{10}$ cm^{-2} ($= 6 \times 10^4$ mIg/cell) and a cell density of $B = 8 \times 10^4$/ml. These parameters agree with estimates for the response of unprimed B cells. The locations and the relative heights of the maxima agree very well with the corresponding experimental curves.

As mentioned above the rising part of the bell-shaped functions in Fig. 11 is determined mainly by the receptor density. Both, its location and its slope change as the receptor density is changed. The decreasing part of the function depends quite sensitively on the assumption of how many receptors must be crosslinked by a single ligand in order to form a stimulatory aggregate. Our calculations indicate that this number should be close to ten, in agreement with the conclusion of Dintzis et al. (1983) that an immunon comprises roughly ten receptors.

Dintzis et al. (1983) have also shown that ligands with valence of less than 10 are able to inhibit the activation achieved by longer ligands. They suggest that such inhibition is due to the formation of small clusters, which in essence rob the larger clusters of receptors and hence reduce the number of stimulatory clusters. With our binding model we are not able to reproduce the inhibition data of Dintzis et al. (1983) indicating that the observed inhibitory phenomenon may *not* be the result of competitive inhibition. In the experiments, inhibition sets in for concentrations of the small inhibitory ligand that are much lower than those required to compete for binding sites effectively with the stimulatory larger ligand.

In vivo cell densities sufficiently high to reach the excess receptor regime can be achieved for almost any type of receptor, especially if the binding affinity is of the order 10^8 M^{-1} or larger, or if the cells are sensitive to signals requiring that a large number of receptors are crosslinked by the same ligand as in the case of the response of T-independent B cells. In the excess receptor regime, the number of ligands bound per cell and, consequently, the number of crosslinks per cell is smaller than in the excess ligand regime that has been explored by most experimental and theoretical studies. If the response is a monotonically increasing function of the number

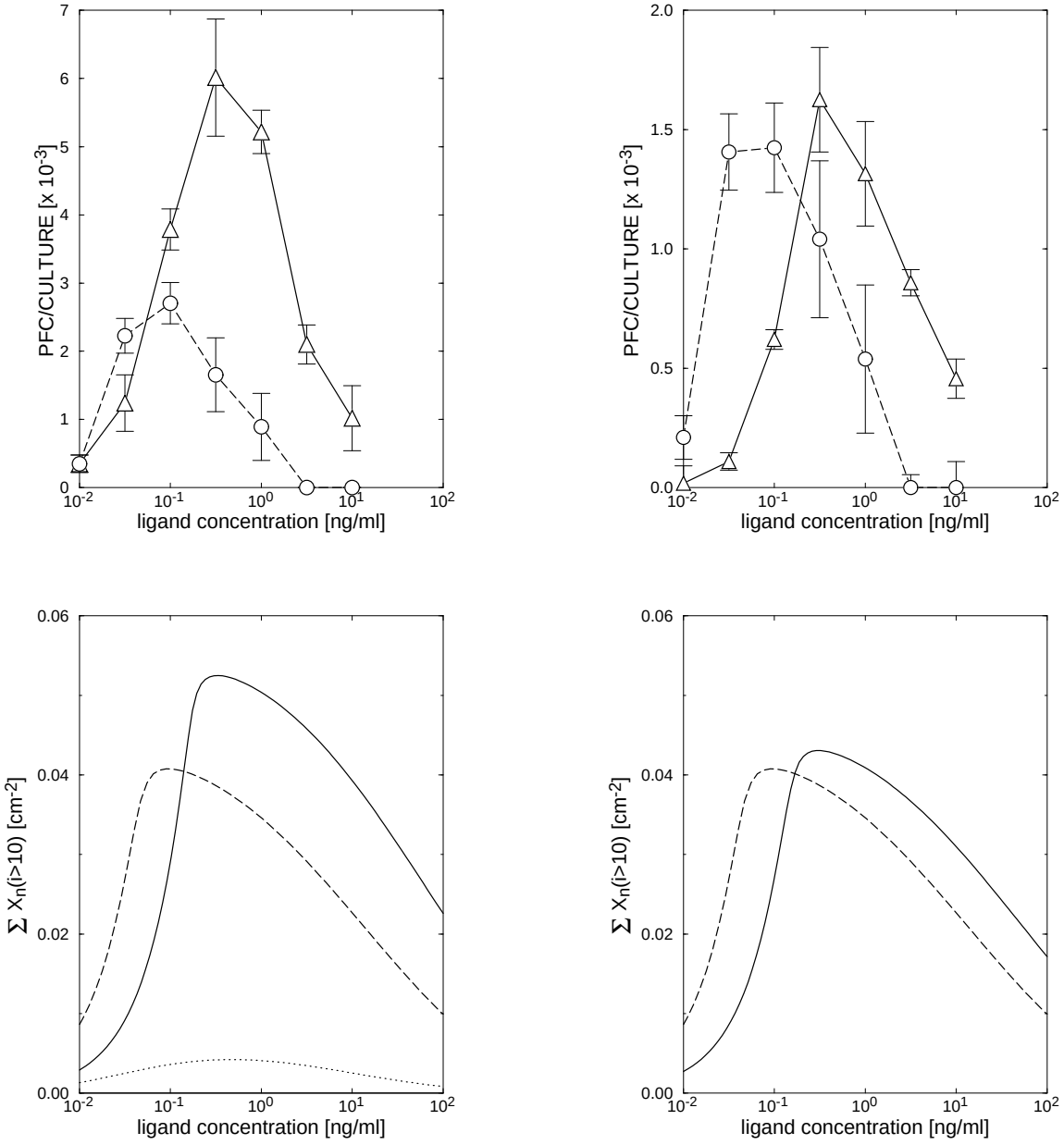

Figure 11: *Concentration of multiply bound ligands on B cells.* The dependence of the fraction of receptor sites in cell-bound ligand states containing more than 10 bound ligand sites upon the ligand concentration shows a qualitatively similar form for ligands of different valencies and different molecular weight. We compare experimental data taken from Dintzis et al. (1983) (top row) with our theoretical results (bottom row). The left panels show the binding of the molecules DI-126 (solid line), D'$_{53}$ (dashed line), B'$_{19}$ (dotted line in the lower panel), and A'$_{11}$ (in the lower panel the concentrations are so small that the plot coincides with the x axis); for B'$_{19}$ and A'$_{11}$ no response is observed in the experiment and we have opted to omit the corresponding data points from the top panel. The right panels show the binding of the molecules DI-59 (solid line) and D'$_{53}$ (dashed line). The parameters for the theoretical curves are: $K_1 = 10^5$ M^{-1}, $R_T = 4 \times 10^{10}$ cm^{-2}, $\kappa_x = 1$, $\alpha = 2.5 \times 10^{-27}$ cm^2 mol, and $B = 8 \times 10^4$/ml.

of crosslinks, then in the excess receptor regime the proliferation of a cell population can cease entirely due to depletion of ligand caused by the population expansion. To our knowledge this

mechanism of cell population control has not been considered previously.

In ligand ensembles with a fixed distribution of ligands of different valencies we find a marked preference for the binding of large ligands both in the excess receptor regime and in the early transition from the excess receptor to the excess ligand regime. In the excess receptor regime (and at very small ligand concentrations irrespective of the receptor density) the binding of individual n-mers, i.e., ligands of size n, do not interfere with one another, since the receptor occupancy is low. Thus, the bound states for each n-mer are the same as if it would bind in the absence of the other ligands. If the crosslinking affinity κ_x is sufficiently large, however, larger ligands will bind more frequently than smaller ones, solely because of the larger number of available binding sites. At ligand concentrations where crosslinking is still frequent but at which ligands start to compete for receptors this preference for binding large ligands becomes even more pronounced. At this point the number of sites bound per ligand, averaged over the entire ensemble, increases even though the average number of sites bound for each n-mer decreases. The global average increases, because the n-mer averages decrease faster for smaller n and because the concentrations of bound large n-mers increase faster than those of bound small ones. At large ligand concentrations, finally, again almost every ligand is bound at only one site. In this situation it does not matter anymore how many sites a ligand has in total and the concentrations of cell-bound n-mers reflect the fixed total concentrations of n-mers.

Receptor density can also have a strong influence on the equilibrium binding properties of ligand ensembles. The smaller the receptor density in the excess receptor regime the larger is the ensemble average of the number of sites bound per ligand indicating preferred binding of increasingly larger ligands.

In vivo ensembles of ligands of different valencies may be formed under numerous circumstances. One example is the *in vivo* formation of aggregates of two kinds of basic units. If one of the basic units carries binding sites for a receptor, aggregates containing different numbers of this basic unit constitute ligands of different valencies for the receptor. Depending on the nature of the aggregating units and the biochemistry of mutual binding among those units we expect to find different kinds of ligand distribution. Let us illustrate this for immune complexes resulting from the binding of antibodies to antigens. Antibodies in immune complexes expose the constant Fc region which is recognized by Fc-receptors on a large number of cell types, e.g., macrophages and follicular dendritic cells. The distribution of the number of Fc regions on an immune complex varies drastically with the valency of both the antigen and the antibodies. Two extreme cases are the aggregation of bivalent antigen by bivalent antibody and the coating by bivalent antibody of a multivalent antigen which is much larger than the antibody as, for instance, a bacterium. In the absence of any cells capable of binding the antigen or the antibody the concentrations of aggregate decrease geometrically with the size of the aggregate in the first case (Goldberg, 1952; DeLisi and Perelson, 1976; Perelson and DeLisi, 1980) and have a normal distribution [??] around the average number of antibodies bound per antigen in the second case. These distributions will change, of course, in the presence of cells carrying receptors for either the antigen or the antibody. Things become even more involved when both the antigen and the antibody can bind to receptors on the *same* cell. Immune complexes, for instance, can bind to antigen-specific B cells either by means of an antigenic determinant binding to membrane-bound immunoglobulins or by means of the antibody Fc region binding to the corresponding Fc-receptor. A discussion of the mutual equilibrium of several kinds of dissolved molecules and cell-bound receptors is beyond the scope of this manuscript.

Acknowledgments

We thank Byron Goldstein for helpful suggestions. This work was done under the auspices of the U.S. Department of Energy and supported by NIH grant RR06555 (A.S.P.) and the Santa Fe Institute through the Josesph P. and Jeanne M. Sullivan Foundation Program in Theoretical Immunology.

Appendix – Average number of sites bound per oligomer for oligomer ensembles in the excess receptor regime

Here we present the derivation of the approximate value Eq. 32 for the average number of sites bound per oligomer $\langle c \rangle_{er}$ for a heterogeneous oligomer ensemble with the composition Eq. 24 in the excess receptor regime.

The average number of sites bound per oligomer in the limit of high cell density ($r = 1$) is given by

$$\langle c \rangle = \frac{\frac{K_1 R}{\kappa_x} \sum_{n=1}^{\infty} X_n(0) \sum_{i=1}^{n} i \binom{n}{i} \kappa_x^i}{\frac{K_1 R}{\kappa_x} \sum_{n=1}^{\infty} X_n(0) \sum_{i=1}^{n} \binom{n}{i} \kappa_x^i} = \tag{A1}$$

$$= \frac{\sum_{n=1}^{\infty} X_n(0) n \kappa_x (\kappa_x + 1)^{n-1}}{\sum_{n=1}^{\infty} X_n(0)[(\kappa_x + 1)^n - 1]} \tag{A2}$$

Using the approximation Eq. 31 for the concentration of free oligomers $X_n(0)$ and evaluating the sums over i we obtain

$$\langle c \rangle \approx \frac{\kappa_x \sum_{n=1}^{n_c} X g^{n-1} n (\kappa_x + 1)^{n-1} + \kappa_x \sum_{n=n_c+1}^{\infty} X g^{n-1} n (\kappa_x + 1)^{n-1} \frac{\kappa_x}{\kappa_1 [(\kappa_x+1)^n - 1]}}{\sum_{n=1}^{n_c} X g^{n-1}[(\kappa_x + 1)^n - 1] + \sum_{n=n_c+1}^{\infty} X g^{n-1}[(\kappa_x + 1)^n - 1] \frac{\kappa_x}{\kappa_1 [(\kappa_x+1)^n - 1]}} = \tag{A3}$$

$$= \kappa_x \frac{\sum_{n=1}^{n_c} n[g(\kappa_x + 1)]^{n-1} + \frac{\kappa_x}{\kappa_1} \sum_{n=n_c+1}^{\infty} n \frac{[g(\kappa_x+1)]^{n-1}}{(\kappa_x+1)^n - 1}}{(\kappa_x + 1) \sum_{n=1}^{n_c} [g(\kappa_x + 1)]^{n-1} - \sum_{n=1}^{n_c} g^{n-1} + \frac{\kappa_x}{\kappa_1} \sum_{n=n_c+1}^{\infty} g^{n-1}} \tag{A4}$$

Summation of the n-mer size n is simple except for the second expression in the numerator. Calculating the simple sums first we obtain

$$\sum_{n=1}^{n_c} n[g(\kappa_x + 1)]^{n-1} = \frac{1 - [n_c + 1 - n_c g(\kappa_x + 1)][g(\kappa_x + 1)]^{n_c}}{[1 - g(\kappa_x + 1)]^2} \tag{A5}$$

$$\sum_{n=1}^{n_c} [g(\kappa_x + 1)]^{n-1} = \frac{1 - [g(\kappa_x + 1)]^{n_c}}{1 - g(\kappa_x + 1)} \tag{A6}$$

$$\sum_{n=1}^{n_c} g^{n-1} = \frac{1 - g^{n_c}}{1 - g} \tag{A7}$$

$$\sum_{n=n_c+1}^{\infty} g^{n-1} = \frac{g^{n_c}}{1 - g} \tag{A8}$$

Using these results the denominator of Eq. A4 becomes

$$(\kappa_x + 1) \sum_{n=1}^{n_c} [g(\kappa_x + 1)]^{n-1} - \sum_{n=1}^{n_c} g^{n-1} + \frac{\kappa_x}{\kappa_1} \sum_{n=n_c+1}^{\infty} g^{n-1} =$$

$$= (\kappa_x + 1) \frac{1 - [g(\kappa_x + 1)]^{n_c}}{1 - g(\kappa_x + 1)} + \left[\left(\frac{\kappa_x}{\kappa_1} + 1 \right) g^{n_c} - 1 \right] \frac{1}{1 - g} \tag{A9}$$

Let us now turn to the non-trivial part, i.e., to the second expression in the numerator in Eq. A4. From each term in the sum over n we split the factor $[1-(\kappa_x+1)^{-n}]^{-1}$ and replace it by its Taylor expansion (note that $|(\kappa_x+1)^{-n}|<1$, for all n)

$$\sum_{n=n_c+1}^{\infty} n\frac{[g(\kappa_x+1)]^{n-1}}{(\kappa_x+1)^n-1} = \sum_{n=n_c+1}^{\infty} \frac{n[g(\kappa_x+1)]^{n-1}}{(\kappa_x+1)^n}\,\frac{1}{1-(\kappa_x+1)^{-n}} \tag{A10}$$

$$= \sum_{n=n_c+1}^{\infty} \frac{n[g(\kappa_x+1)]^{n-1}}{(\kappa_x+1)^n}\,\sum_{k=0}^{\infty}(-1)^k\frac{1}{(\kappa_x+1)^{nk}} \tag{A11}$$

After exchanging the summations we perform the sum over n which leads to

$$\sum_{n=n_c+1}^{\infty} n\frac{[g(\kappa_x+1)]^{n-1}}{(\kappa_x+1)^n-1}$$

$$= \sum_{k=0}^{\infty}\frac{(-1)^k}{(\kappa_x+1)^{k+1}}\,(\kappa_x+1)^k\,\frac{(\kappa_x+1)^k+[(\kappa_x+1)^k-g]n_c}{[(\kappa_x+1)^k-g]^2}\left[\frac{g}{(\kappa_x+1)^k}\right]^{n_c} \tag{A12}$$

We treat $k=0$ and $k>0$ separately

$$\sum_{n=n_c+1}^{\infty} n\frac{[g(\kappa_x+1)]^{n-1}}{(\kappa_x+1)^n-1}$$

$$= \frac{g^{n_c}}{\kappa_x+1}\left\{\frac{1+(1-g)n_c}{(1-g)^2} + \sum_{k=1}^{\infty}\left[\frac{-1}{(\kappa_x+1)^{n_c}}\right]^k\,\frac{(\kappa_x+1)^k+[(\kappa_x+1)^k-g]n_c}{[(\kappa_x+1)^k-g]^2}\right\} \tag{A13}$$

In the sum over k we neglect g which is usually much less than 1 and becomes more and more negligable with respect to $(\kappa_x+1)^k$ as k increases.

$$\sum_{n=n_c+1}^{\infty} n\frac{[g(\kappa_x+1)]^{n-1}}{(\kappa_x+1)^n-1}$$

$$= \frac{g^{n_c}}{\kappa_x+1}\left\{\frac{1+(1-g)n_c}{(1-g)^2} + \sum_{k=1}^{\infty}\left[\frac{-1}{(\kappa_x+1)^{n_c}}\right]^k\,\frac{(\kappa_x+1)^k(n_c+1)}{(\kappa_x+1)^{2k}} + \Omega\right\} \tag{A14}$$

$$\approx \frac{g^{n_c}}{\kappa_x+1}\left\{\frac{1+(1-g)n_c}{(1-g)^2} + \sum_{k=1}^{\infty}\left[\frac{-1}{(\kappa_x+1)^{n_c}}\right]^k\,\frac{(\kappa_x+1)^k(n_c+1)}{(\kappa_x+1)^{2k}}\right\} \tag{A15}$$

We comment on the error Ω below. The sum over k can now easily be calculated and we obtain

$$\sum_{n=n_c+1}^{\infty} n\frac{[g(\kappa_x+1)]^{n-1}}{(\kappa_x+1)^n-1} = \frac{g^{n_c}}{\kappa_x+1}\left\{\frac{1+(1-g)n_c}{(1-g)^2} + \frac{n_c+1}{(\kappa_x+1)^{n_c+1}-1}\right\} \tag{A16}$$

We insert Eqs. A5, A16, and A9 into Eq. A4 and obtain the result Eq. 32.

When we omit g in the step from Eq. A14 to Eq. A15 we commit the error

$$\Omega = \sum_{k=1}^{\infty}\left[\frac{-1}{(\kappa_x+1)^{n_c}}\right]^k\left[\frac{(\kappa_x+1)^k(n_c+1)-n_cg}{[(\kappa_x+1)^k-g]^2} - \frac{(\kappa_x+1)^k(n_c+1)}{[(\kappa_x+1)^k]^2}\right] \tag{A17}$$

$$= (n_c+2)g\,\sum_{k=1}^{\infty}\left[\frac{-1}{(\kappa_x+1)^{n_c+2}}\right]^k\frac{1-\nu\gamma_k}{(1-\gamma_k)^2} \tag{A18}$$

with

$$\nu \;=\; \frac{n_c+1}{n_c+2} \qquad \text{and} \qquad \gamma_k \;=\; \frac{g}{(\kappa_x+1)^k} \tag{A19}$$

A crude estimates yields that Ω is bounded by

$$\frac{-[n_c+2]g}{[(\kappa_x+1)^{n_c}-(\kappa_x+1)^{-(n_c+4)}]} \;<\; \Omega \;<\; \frac{[n_c+2]g}{[(\kappa_x+1)^{2(n_c+1)}-1]} \tag{A20}$$

The relative error

$$\omega \;=\; \Omega\left\{\frac{1+(1-g)n_c}{(1-g)^2} \;+\; \frac{n_c+1}{(\kappa_x+1)^{n_c+1}-1}\right\}^{-1} \tag{A21}$$

is bounded by

$$\frac{-[n_c+2][1-g]^2 g}{[1+(1-g)n_c][(\kappa_x+1)-g]^2[\kappa_x+1]^{n_c}} \;<\; \omega \;<\; \frac{[n_c+2][1-g]^2 g}{[1+(1-g)n_c][(\kappa_x+1)-g]^2[\kappa_x+1]^{2(n_c+1)}} \tag{A22}$$

where the dominant factors are $(\kappa_x+1)^{-n_c}$ for the lower and $(\kappa_x+1)^{-2(n_c+1)}$ for the upper bound, unless both n_c and κ_x are small.

REFERENCES

DeLisi, C. and A. S. Perelson. 1976. The kinetics of aggregation phenomena. I. Minimal models for patch formation on lymphocyte membranes. *J. theor. Biol.* 62:159 – 210.

Dembo, M. and B. Goldstein. 1978. Theory of equilibrium binding of symmetric bivalent haptes to cell surface antibody: Application to histamine release from basophils. *J. Immunol.* 121:345 – 353.

Dembo, M., A. Kagey-Sobotka, L. M. Lichtenstein, and B. Goldstein. 1982. Kinetic analysis of histamine release due to covalently linked IgE dimers. *Mol. Immunol.* 19:421 – 434.

Dintzis, H. M., R. Z. Dintzis, and B. Vogelstein. 1976. Molecular determinants of immunogenicity: The immunon model of immune response. *Proc. Natl. Acad. Sci. USA* 73:3671 – 3675.

Dintzis, R. Z., M. H. Middleton, and H. M. Dintzis. 1983. Studies on the immunogenicity and tolerogenicity of T-independent antigens. *J. Immunol.* 131:2196 – 2203.

Dower, S. A., C. DeLisi, J. A. Titus, and D. M. Segal. 1981. Mechanism of binding of multivalent immune complexes to Fc receptors. I. Equilibrium binding. *Biochem.* 20:6326 – 6334.

Dower, S. K., J. A. Titus, and D. M. Segal. 1984. The binding of multivalent ligands to cell surface receptors. *In* Cell surface dynamics: Concepts and models. A. S. Perelson, C. DeLisi, and F. W. Wiegel, editors. Marcel Dekker:New York. 277 – 328.

Fewtrell, C. and H. Metzger. 1980. Larger oligomers of IgE are more effective than dimers in stimulating rat basophilic leukemia cells. *J. Immunol.* 125:701 – 710.

Gandolfi, A., M. A. Giovenco, and R. Strom. 1978. Reversible binding of multivalent antigen in the control of B lymphocyte activation. *J. Theoret. Biol.* 74:513 – 521.

Goldberg, R. J. 1952. A theory of antibody-antigen reactions. I. Thery for reactions of multivalent antigen with bivalent and univalent antibody. *J. Am. Chem. Soc.* 74:5715 – 5725.

Guyre, P. M., P. M. Morganelli, and R. Miller. 1983. Recombinant immune interferon increases immunoglobulin G Fc receptors on cultured human mononuclear phagocytes. *J. Clin. Invest.* 72:393 – 397.

Kagey-Sobotka, A., M. Dembo, B. Goldstein, H. Metzger, and L. M. Lichtenstein. 1981. Qualitative characteristics of histamine release from human basophils by covalently cross-linked IgE. *J. Immunol.* 127:2285 – 2291.

Kent, U. M., S.-Y. Mao, C. Wofsy, B. Goldstein, S. Ross, and H. Metzger. 1994. Dynamics of signal transduction after aggregation of cell-surface receptors: Studies on the type I receptor for IgE. *Proc. Natl. Acad. Sci. USA* 91:3087 – 3091.

Miale, J. B. 1982. Laboratory medicine. Hematology. St. Louis:MI, 6. edition.

Perelson, A. S. and C. DeLisi. 1980. Receptor clustering on a cell surface. I. Theory of receptor cross-linking by ligands bearing two chemically identical functional groups. *Math. Biosciences* 48:71 – 110.

Perelson, A. S. 1981. Receptor clustering on a cell surface. III. Theory of receptor cross-linking by multivalent ligands: Description by ligand states. *Math. Biosci.* 53:1 – 39.

Perelson, A. S. 1984. Some mathematical models of receptor clustering by multivalent ligands. *In* Cell surface dynamics: Concepts and models. A. S. Perelson, C. DeLisi, and F. W. Wiegel, editors. Marcel Dekker:New York. 223 – 275.

Phillips, N. E. and D. C. Parker. 1983. Fc-dependent inhibition of mouse B cell activation by whole anti-μ antibodies. *J. Immunol.* 130:602 – 606.

Phillips, N. E. and D. C. Parker. 1984. Cross-linking of B lymphocyte Fcγ receptors and

membrane immunoglobulin inhibits anti-immunoglobulin-induced blastogenesis. *J. Immunol.* 132:627 – 632.

Ravetch, J. V. and J. P. Kinet. 1991. Fc receptors. *Annu. Rev. Immunol.* 9:457 – 492.

Segal, D. M., J. D. Taurog, and H. Metzger. 1977. Dimeric immunoglobulin E serves as a unit signal for mast cell degranulation. *Proc. Natl. Acad. Sci. USA* 74:2993 – 2997.

Strand, F. L. 1978. Physiology. New York,NY.

van de Winkel, J. G. J. and P. J. A. Capel. 1993. Human IgG Fc receptor heterogeneity: molecular aspects and clinical implications. *Immunol. Today* 14:215 – 221.

Vogelstein, B., R. Z. Dintzis, and H. M. Dintzis. 1982. Specific cellular stimulation in the primary immune response: A quantized model. *Proc. Natl. Acad. Sci. USA* 79:395 – 399.

Wofsy, C. and B. Goldstein. 1990. Cross-linking of Fc_γ receptors and surface antibodies. *J. Immunol.* 145:1814 – 1825.